



Effects of Annealing on the Microstructures and Mechanical Properties of Cold-Rolled TB8 Alloy

Bingyu Qian, Li Li, Jianfeng Sun, Ruizhi Wu, and Milin Zhang

(Submitted October 5, 2018; in revised form March 16, 2019; published online May 7, 2019)

The microstructure and mechanical properties of TB8 cold-rolled plate with a thickness reduction of 50% during annealing at different temperatures are investigated. The results show that annealing for 1 h below 750 °C does not induce the recrystallization transition, remaining the main texture components of $\{001\} <110>$, $\{113\} <110>$ and $\{112\} <110>$. The ellipsoidal ω phase is formed when the alloy is annealed at 400 °C. α phase is formed when the alloy is annealed from 450 to 750 °C. The size and volume fraction of α phase increases first and then declines in control of driving force of phase transformation and diffusion. The synergistic effect of the precipitation of ω phase and α phase and the disappearance of dislocation makes the tensile strength of the plate decrease first, then increase, and finally decrease with the increase in annealing temperature. The change in plasticity is opposite to that of strength.

Keywords electron microscopy, heat treatment, titanium, x-ray

1. Introduction

Titanium alloys have widespread applications in aerospace, chemical and biomedical industries thanks to their advantages of mechanical properties, corrosion resistance, crack propagation resistance and bio-compatibility properties (Ref 1-5). Titanium alloys are usually classified as α , $\alpha + \beta$ and β alloys, according to the percentage composition of alloying elements (Ref 6). The body-centered cubic (bcc) β matrix can be obtained due to a higher molybdenum equivalent by solid solution and water quenching. During aging, the secondary phases will precipitate, which leads to a significant increase in strength (Ref 7). TB8 is a meta-stable beta titanium alloy with a high specific strength, a good cold formability, and an excellent oxidation resistance as well as thermal stability (Ref 8). The positive specific properties make the alloy widely be used in both the aerospace, automotive industries and bioimplant industries.

Much literature focused on the relationship between tensile properties and microstructure of TB8 alloys (Ref 6, 9-13). Meanwhile, the microstructure evolution during aging treatment has been proposed (Ref 8, 11, 14, 15). The microstructure of near β Ti alloys is highly sensitive to original microstructure and treatment process. Neither phase transformation controlling nor microstructure prediction of the near β Ti alloys has been clearly understood since the discovery of the alloys (Ref 16).

Bingyu Qian, Li Li, and Jianfeng Sun, College of Materials Science and Engineering, Heilongjiang University of Science and Technology, Harbin 150022, People's Republic of China; and **Ruizhi Wu and Milin Zhang**, Key Laboratory of Superlight Materials and Surface Technology, Ministry of Education, College of Materials Science and Chemical Engineering, Harbin Engineering University, Harbin 150001, People's Republic of China. Contact e-mails: sunwind_01@163.com and rzwu@hrbeu.edu.cn.

The microstructure and texture evolution play a paramount role in determining the mechanical properties. The rolling process has been widely utilized in meta-stable β titanium alloy for manufacturing fasteners and composite materials (Ref 17). In TB8 alloy, the evolution of texture and microstructure during cold rolling results in orientation rotation and dislocation multiplication, which can further alter their phase transformation behaviors and mechanical properties during annealing. Thus, it is crucial to study the microstructure evolution of cold-rolled TB8 alloy during annealing. According to our previous studies (Ref 1), the cold-rolled plates consist of only β phase; the grains elongated along the rolling direction. The ultimate tensile strength is 1127 MPa and the elongation is 12.2% with the thickness reduction of 50%. Meanwhile, the textures change from initial $\{110\} <001>$ and $\{113\} <332>$ to α -fiber components and $\{001\} <110>$ orientation after cold rolling with a thickness reduction of 50%. However, there are few investigations dealing with the annealing microstructure and textures of β -Ti alloys (Ref 18). The present study focuses on cold-rolled TB8 titanium alloy, with the aim to understand the phase transformation mechanisms through investigating the microstructure evolution at different annealing temperatures. The effect of microstructure on the mechanical properties is also discussed.

2. Materials and Experimental Methods

The chemical composition of TB8 alloy is Ti-15.08 wt.%Mo-2.91 wt.%Al-2.72 wt.%Nb-0.18 wt.%Si. The cold-rolled TB8 alloy plate with a total thickness reduction of 50% and the final thickness of 3 mm was employed, which were cold-rolled from the hot-rolled plates with a thickness of 6 mm. The microstructure of the cold-rolled TB8 plate is shown in Fig. 1. It is apparent that the fiber-like microstructure is clear along the longitudinal direction. Annealing was conducted at temperatures ranging from 300 to 800 °C for 1 h in a preheated air furnace and followed by air cooling.

The specimens were then polished and chemically etched in a solution of 10 vol.% HF, 10 vol.% HNO₃ and 80 vol.% H₂O.

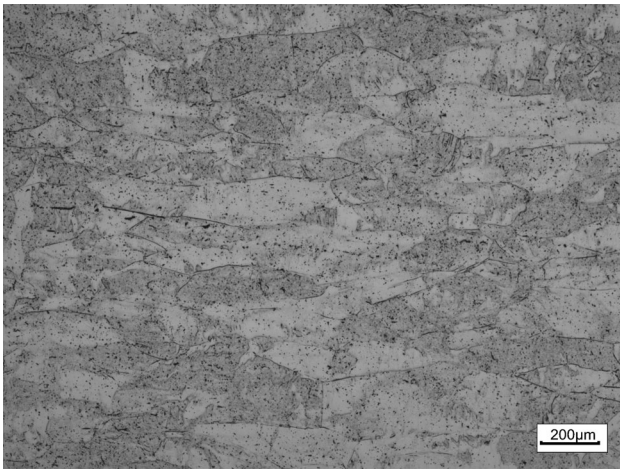


Fig. 1 Microstructure of the TB8 cold-rolled plate

Microstructure characterization was observed by Axio Scope A1 optical microscope (OM) and Camscan MX2600 FE scanning electron microscopy (SEM). Quantitative analysis of α phase was calculated by using Photoshop and ImageJ softwares. X-ray diffraction measurements were carried out at room temperature with Cu K α , 35 kV and 100 mA. Textures were measured from the mid-thickness sections of the specimens using an x-ray texture goniometer (PANalytical X'Pert Pro MPD) with Co K α radiation based on Schulz reflection technique. {200}, {211} and {110} of β phase were measured, and the corresponding incomplete pole figures were obtained. Orientation distribution functions (ODFs) were calculated using the incomplete pole figures. For further investigation, JEM-2100 transmission electron microscope (TEM) was used to examine the microstructure of specimens. Thin plate with the thickness of 1 mm was cut along the rolling direction and then ground using abrasive paper to the thickness of 30 μ m, and then, 3 mm disks were thinned by ion milling. The electron backscatter diffraction (EBSD) was performed using the INCA Crystal EBSD.

Tensile specimens with gauge dimensions of 25 \times 5 \times 1 mm were prepared. The tensile specimens were ground and polished before testing. Tensile tests were carried out on INSTRON-5569 testing machine at room temperature with a strain rate of $1 \times 10^{-3} \text{ s}^{-1}$. Three tests were performed for each sample.

3. Results

3.1 Mechanical Properties during Annealing

Figure 2 shows the influence of annealing temperature on mechanical properties of cold-rolled TB8 alloy. The variations of mechanical properties during annealing can be divided into three stages. In the first stage, with the increase in annealing temperature from the cold-rolled state to 350 $^{\circ}\text{C}$, the ultimate tensile strength decreases from 1127 to 1063 MPa. The elongation is found to increase from 12.2 to 16.9%. In the second stage, annealing in the range of 400–550 $^{\circ}\text{C}$, the strength is higher than that of the cold-rolled TB8 alloy. The strength is 1170 MPa, the elongation drops to 9.56% at 400 $^{\circ}\text{C}$, and the strength upgrades to 1373 MPa, the elongation is

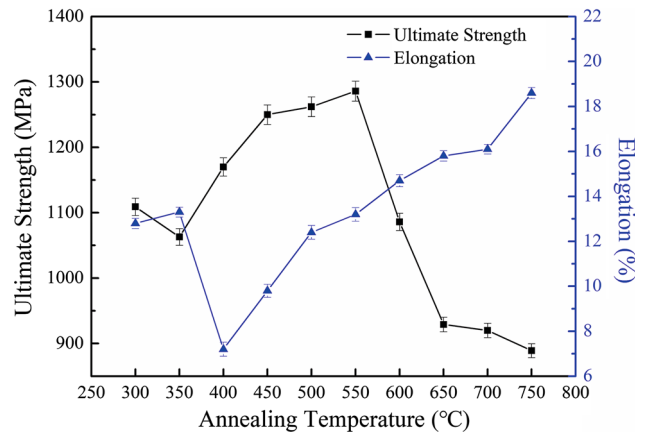


Fig. 2 The relationship between mechanical properties and annealing temperature of TB8 cold-rolled plates

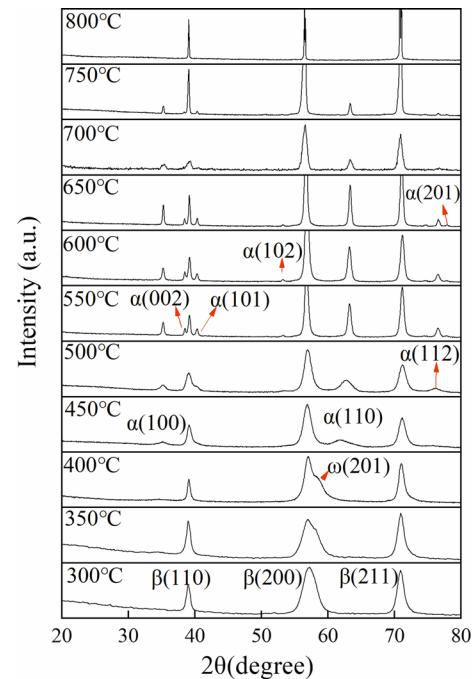


Fig. 3 XRD pattern of the TB8 cold-rolled plate after annealing treated from 300 to 800 $^{\circ}\text{C}$ for 1 h

11.56% at 450 $^{\circ}\text{C}$. This may be attributed to the precipitation of ω phase. After annealing at 550 $^{\circ}\text{C}$, the strength is 1286 MPa, and the elongation recovers to 14.49%. It may be explained that there is α phase precipitation and the work hardening caused by cold rolling deformation is not eliminated. In the third stage, with the increase in annealing temperature from 600 to 750 $^{\circ}\text{C}$, the tensile strength decreases and the elongation increases, showing an obvious softening process.

3.2 XRD Analysis

Figure 3 presents the XRD patterns of the TB8 cold-rolled plate after annealing from 300 to 800 $^{\circ}\text{C}$ for 1 h. The plates consist of only β phase after annealing at 300 and 350 $^{\circ}\text{C}$, which is the same as the cold-rolled state. The width of diffraction peaks is broadened due to the lattice distortion indicating that the annealing temperature is not high enough to

cause significant phase transformation, and the internal stress is not eliminated (Ref 19). The ω (201) peak is detected after annealing at 400 °C, showing that $\beta \rightarrow \omega$ transformation occurs, which will reduce the plasticity of the material (Ref 20). α phase appears at 450 °C, with the increase in temperature, the diffraction peaks of α phase become stronger and more α peaks appear, which illustrates that α phase fraction increases. Whereas when the temperature is higher than 650 °C, α peaks become weak. Furthermore, only single β phase peaks exist when the temperature is up to 800 °C.

From the thermodynamics of phase transition, the driving force of $\beta \rightarrow \alpha$ phase transition during annealing is the Gibbs free energy difference between the two phases (Ref 21). When the temperature is low, the difference of Gibbs free energy between two phases is large resulting in large driving force of phase transition, which promotes the nucleation of α phase. The free energy difference between the two phases decreases as the temperature rises, and the driving force of phase transition decreases. Accordingly, the formation of α phase is prevented. Nevertheless, according to the phase transformation kinetic, $\beta \rightarrow \alpha$ phase transition proceeds as a diffusion reaction. The increase in temperature increases the diffusion rate and promotes the formation of α phase. In a certain temperature range, the amount of α phase increases with the increase in temperature. When the temperature rises to a certain extent, the amount of α phase decreases. Therefore, the amount of α phase is affected by these two factors, which increases then decreases with the increase in temperature. The nose temperature of $\beta \rightarrow \alpha$ transition of cold-rolled alloy is about 600-650 °C, as can be seen from Fig. 3. In addition, the width of diffraction peak becomes narrow, which presages that the manifest recovery occurring leads to the eliminations of lattice distortion and internal stress. Compared with the diffraction peaks at 750 °C, the peaks become narrower except for the disappearance of α phase at 800 °C. The internal stress is further eliminated, foreshowing recrystallization may take place at this temperature.

3.3 Microstructure

Figure 4 depicts the microstructure of cold-rolled TB8 alloy annealed from 300 to 800 °C for 1 h. The microstructure is composed of single β phase grains and still retains the elongated morphology produced by cold rolling deformation when annealed at 300 and 350 °C as shown in Fig. 4(a) and (b). That is, the microstructure does not change evidently due to the low annealing temperature.

XRD analysis (Fig. 3) shows that ω phase precipitates when annealed at 400 °C. In Fig. 4(c), ω phase cannot be observed due to the small size of ω phase. The grain is still elongated when annealed below 650 °C (Fig. 4c-h), indicating that recrystallization transformation does not take place in this temperature range. As well, more and more black region in the microstructure are observed in this temperature range. Combined with the analysis of Fig. 3, it can be concluded that, with the increase of temperature, the volume fraction of α phase becomes more and more. When annealing at 700 °C (Fig. 4i), the deformation structure still exists, but the grain boundaries become straight, revealing that cold-rolled plate has completed recovery process. Annealing at 750 °C, as shown in Fig. 4(j), the microstructure still retains the deformation morphology, and there is no obvious grain growth, but there are some fine equiaxed grains (red circled area). It is indicated that partial

recrystallization occurs. Figure 4(k) demonstrates that the elongated grains change into equiaxed grains when the temperature rises to 800 °C, and the recrystallization process is completed. It shows that the temperature of complete recrystallization is between 750 and 800 °C.

The SEM morphologies of the samples annealed from 450 to 750 °C are shown in Fig. 5. After annealing at 450 °C, the α phase cannot be observed because of its small number and size, shown in Fig. 5(a). Annealing at 500 °C, fine and lenticular precipitates form at inner defects such as dislocations and vacancies. Annealing at 550 °C resulted in more α particles nucleating and that some nucleated α precipitates grow into needle-like morphology in the β matrix, as displayed in Fig. 5(c). Increasing the temperature to 600 °C, finer acicular α phases form in the grain. A marked increase in the size and volume fraction of α precipitate is observed after annealing at 650 °C (Fig. 5d); α precipitates are much coarser and more uniformly dispersed than that corresponding to lower annealing temperature. The size of acicular α phase increases further, and spherical α phase appears, while the volume fraction decreases when annealed at 700 °C. After annealing at 750 °C, the α phase is further spheroidized and the volume fraction is further reduced as shown in Fig. 5(g). There is only a little of precipitation and the linked dot α phase formed annealing at low temperature (Fig. 5a-c). After a higher temperature annealing, the precipitation grows up to acicular morphology, shown as Fig. 5(d), (e) and (f). This is due to the deformation band and sub-grains in the β grain result in the inhomogeneous α nucleation. The slow diffusion element Mo leads to an increased precipitation driving force, which makes the alpha phase nucleate in the defect, which is also an important factor (Ref 22). When the annealing temperature is higher than 700 °C, which approached the phase transformation temperature, the driving force decreases, but the diffusion increases, resulting in the formation of spheroidization α .

The characteristics of the α length and width, volume fraction of α were quantitatively counted and the results are displayed in Table 1. It can be seen that when the annealing temperature increases, the length and width of α phase increase, the volume fraction increases first and then decreases, and the spherical α phase appears when the temperature exceeds 700 °C. The volume fraction increases from 9.66% after 500 °C to over 79% of 650 °C and then decreased to 33.2% of 700 °C and 8.47% of 750 °C. The size, quantity and distribution of α phase play an important role in the strengthening effect, which acts as a mainly strengthening phase in β titanium alloy. Fine, dispersed and uniformly distributed α phase is beneficial to improve the comprehensive properties of the alloy. The strength can be expressed by the following rule of mixture (Ref 23, 24):

$$\sigma = \text{function of } (f\alpha_p l/d\alpha_p + f\alpha_s l/d\alpha_s) \quad (\text{Eq 1})$$

where σ is the yield strength, $f\alpha_p$ the area fraction of α_p phase (primary α) and $f\alpha_s$ is the area of α_s phase (secondary α), $d\alpha_p$ is the size of α_p , $d\alpha_s$ is the size of α_s phase. It can be seen that the increase in the volume fraction of α_p and α_s or decrease in the size of α_p and α_s will improve yield strength. In case of lower annealing temperatures, the α precipitates with a very small size lead to a quite high yield strength. At higher aging temperatures, the α_s phase coarsening results in a reduction in strength.

The appearance of ω phase will reduce the plasticity of the alloy. Figure 6(a) shows diffraction pattern on the $[\bar{1}\bar{1}0]_\beta$ zone,

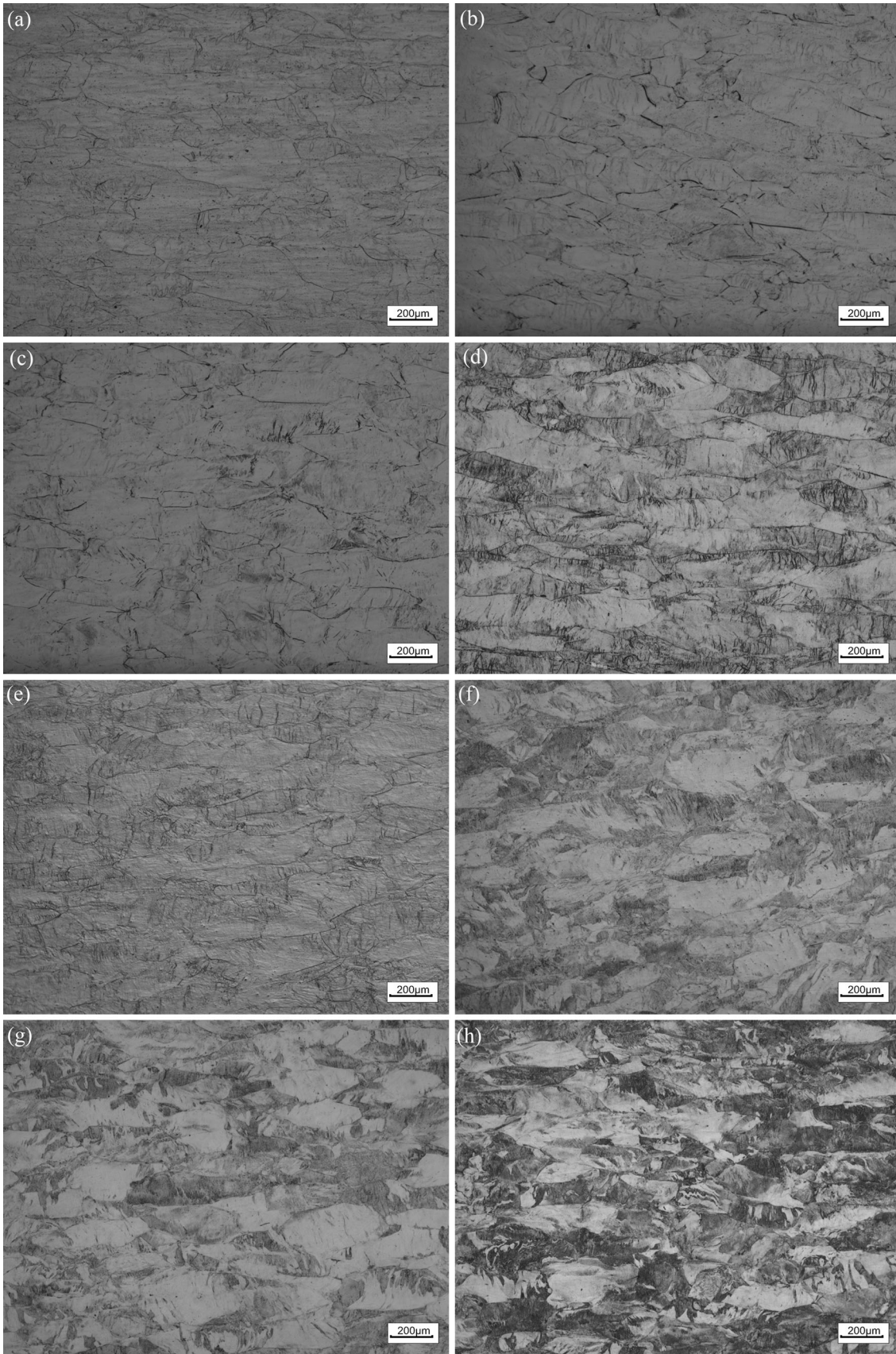


Fig. 4 Microstructure of the TB8 cold-rolled plate annealed at (a) 300 °C, (b) 350 °C, (c) 400 °C, (d) 450 °C, (e) 500 °C, (f) 550 °C, (g) 600 °C, (h) 650 °C, (i) 700 °C, (j) 750 °C and (k) 800 °C (Color figure online)

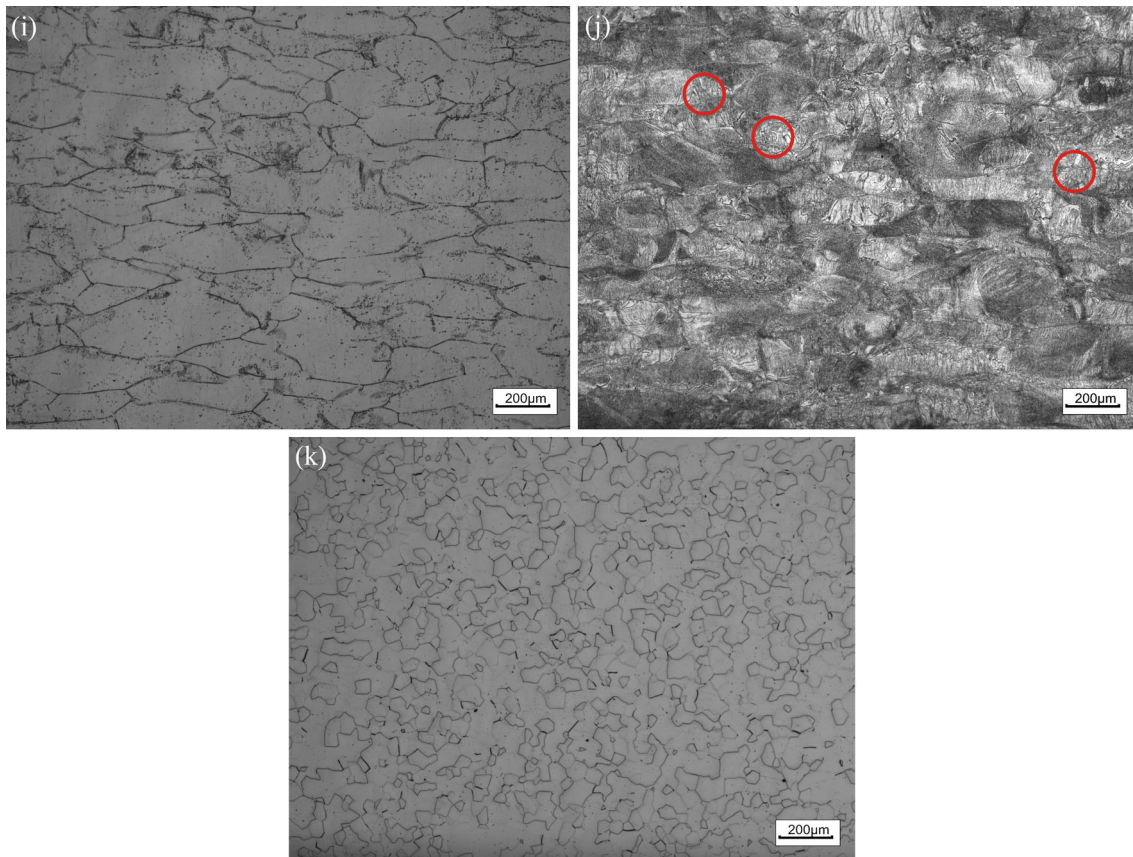


Fig. 4 continued

and Fig. 6(b) shows dark field image acquired from the reflections indicated in Fig. 6(a). The ellipsoid ω phase with the size of 30-50 nm distributes uniformly in the matrix can be observed annealed at 400 °C, which indicates that a small mismatch between ω phase and matrix (Ref 25, 26). The orientation relationship between β matrix and ω phase is $\langle \bar{1}\bar{1}0 \rangle_{\beta} // \langle 11 \bar{2}0 \rangle_{\omega}$ and $(1 \bar{1}2)_{\beta} // (1 \bar{1}00)_{\omega}$, as shown in Fig. 6(b), which is consistent with the orientation relationship between ω phase and β phase in most titanium alloys (Ref 27-30). Li et al. reported that, the isothermal ω phase firstly forms through shearing mechanism. Then $\{111\}$ plane of β phase collapses to form ω phase nuclei. Accordingly, the ω phase formed during annealing maintains a certain orientation relationship with the β phase (Ref 20).

Figure 7(a) shows TEM imaging for cold-rolled TB8 alloy annealing at 450 °C. About 200-350 nm acicular α phase distributes in β matrix. The white circle indicates that there is ω phase in the microstructure, and the size of ω phase is larger than that of annealed at 400 °C. Figure 6(b) shows a $[113]_{\beta}$ zone axis electron diffraction pattern. Comparing with the pattern shown in Fig. 5(b), it is evident that, in addition to the ω reflections present at $1/3$ and $2/3$ $\{112\}$ β locations, there are additional reflections located near the $1/2$ $\{112\}$ β locations. Previous reports suggest that these additional reflections arised from fine-scale α precipitates present in the β matrix of Ti alloys (Ref 31-33).

The original structure of cold-rolled plate is single β phase. Figure 8 shows the TEM morphology of cold-rolled TB8 alloy before annealing. A large number of dislocations exist and entangle which provide favorable positions for the nucleation

of α phase and ameliorate the formation of α phase. It can be seen from Fig. 7(a) that many dislocations exist around α phase, marked by the red ellipse, which further indicates that the dislocation provides a favorable position for the nucleation of α phase.

Figure 9 presents the EBSD grain diagram of the annealed alloy at 700 °C. Figure 9(a) describes the grain orientation above 2° and Fig. 9(b) shows the grain orientation above 15°. Comparing the two graphs, the grain boundaries of some large angle grains and the sub-grain boundaries become straight such as the position shown by the white arrow. This also proves that the obvious recovery process occurs during tempering. In addition, many small angle sub-grains are found in the large angle grains, such as shown in the white circle. Tens of thousands of dislocations exist in cold-rolled plates (as shown in Fig. 8). The decrease in grain boundary energy is a spontaneous process. With the increase in annealing temperature, the dislocations slip and meet with each other resulting in the decrease of dislocation density. The further movement of dislocations makes the dislocations vertically align to form sub-grain boundaries, completing the process of polygonalization and eventually leading to the straightening of grain boundaries.

Figure 10(a) and (b) shows the morphology of dislocation annealing at 300 and 750 °C, respectively. Compared with the cold-rolled state (as shown in Fig. 8), the dislocation density of TB8 alloy annealing at 300 °C has no significant change due to the dislocation motion is not fully activated at low annealing temperature. However, the dislocation density decreases sharply to form dislocation cell structure when annealed at 750 °C due to dislocation slipping and climbing. The decrease

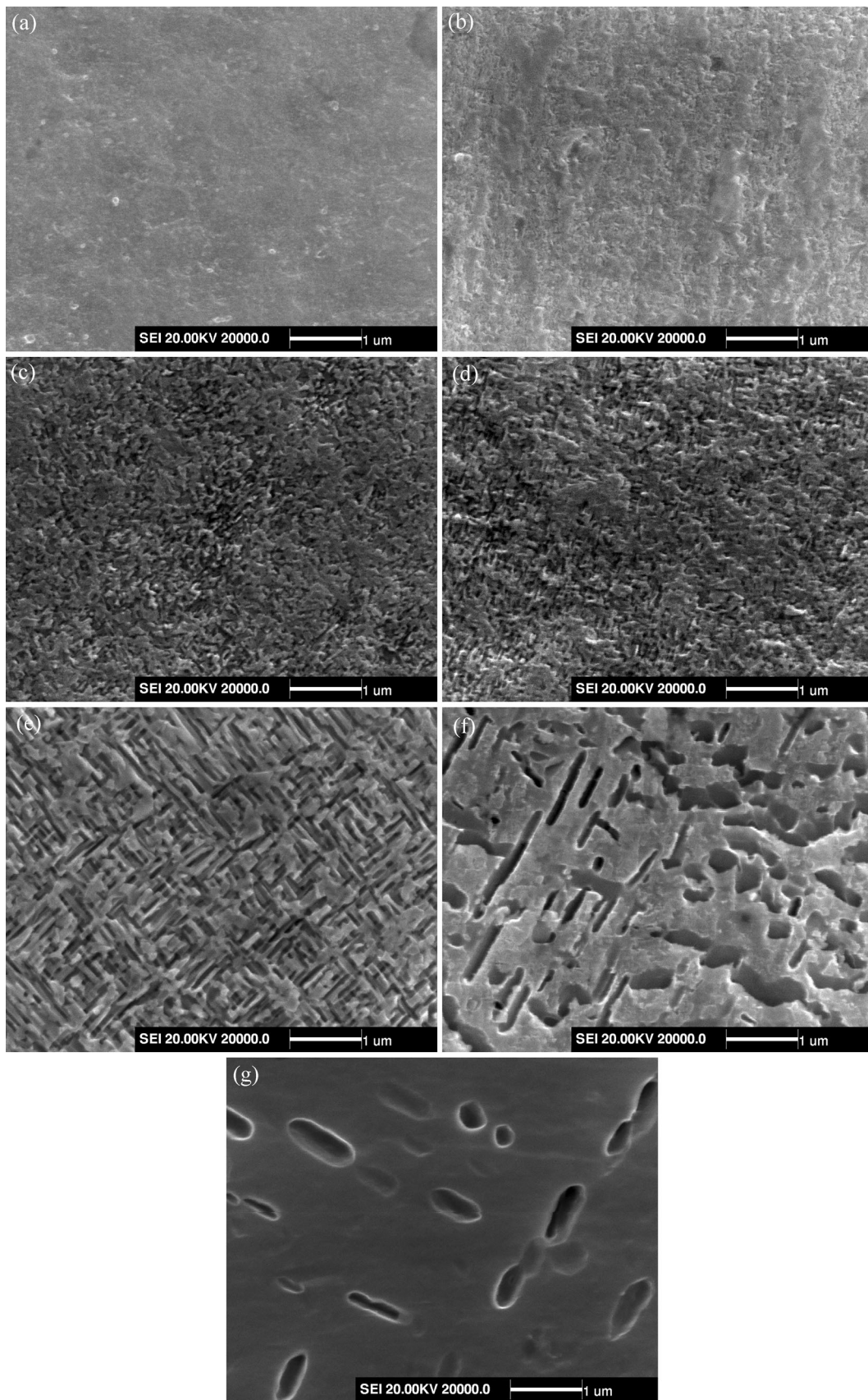


Fig. 5 The SEM morphologies of the TB8 cold-rolled plate annealed at (a) 450 °C, (b) 500 °C, (c) 550 °C, (d) 600 °C, (e) 650 °C, (f) 700 °C, (g) 750 °C

Table 1 The microstructural parameters of the TB8 alloy annealed at different temperature

Annealing temperature, °C	Average α width, μm	Average α length, μm	Volume fraction of α , %
500	0.028	0.071	9.66
550	0.061	0.117	32.7
600	0.089	0.183	42.3
650	0.114	0.601	79.8
700	0.146	0.860	33.2
750	0.267	0.756	8.47

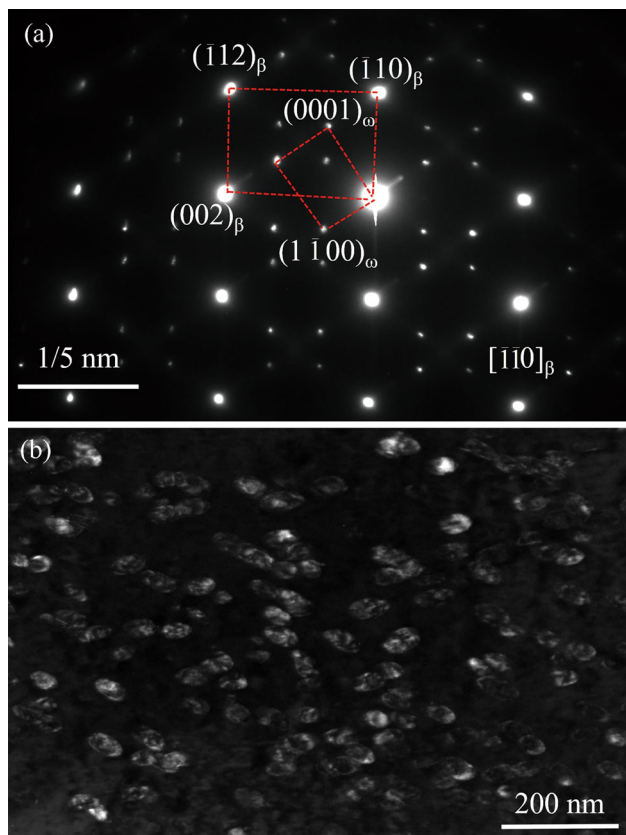


Fig. 6 (a) The selected area electron diffraction pattern of $[\bar{1}\bar{1}\bar{0}]_{\beta}$ zone annealed at 400 °C for 1 h and (b) dark field image acquired from the reflections indicated in Fig. 6(a)

in α phase and defects reduces the strength of the material and improves the plasticity.

Figure 11 shows section ($\varphi_2 = 45^\circ$) of the orientation distribution functions (ODFs) of cold-rolled plates after annealing at 700 °C for 1 h. There are $\{001\} \langle 110 \rangle$, $\{113\} \langle 110 \rangle$ and $\{112\} \langle 110 \rangle$ components. The $\{001\} \langle 110 \rangle$ and $\{112\} \langle 110 \rangle$ components are weakened, while the $\{113\} \langle 110 \rangle$ is strengthened by comparison to cold-rolled state shown in Ref 1. This indicates that the change in mechanical properties during annealing is independent of texture evolution.

There is no obvious phase transition during annealing at 300-350 °C; therefore, the main factor affecting the mechanical properties of the alloy is the elimination of the internal stress during the annealing. The strength decreases slightly and the elongation increases slightly with the increase of temperature. When the annealing temperature is 400 °C, ω phase is formed in the microstructure (Fig. 6b), which increases the strength,

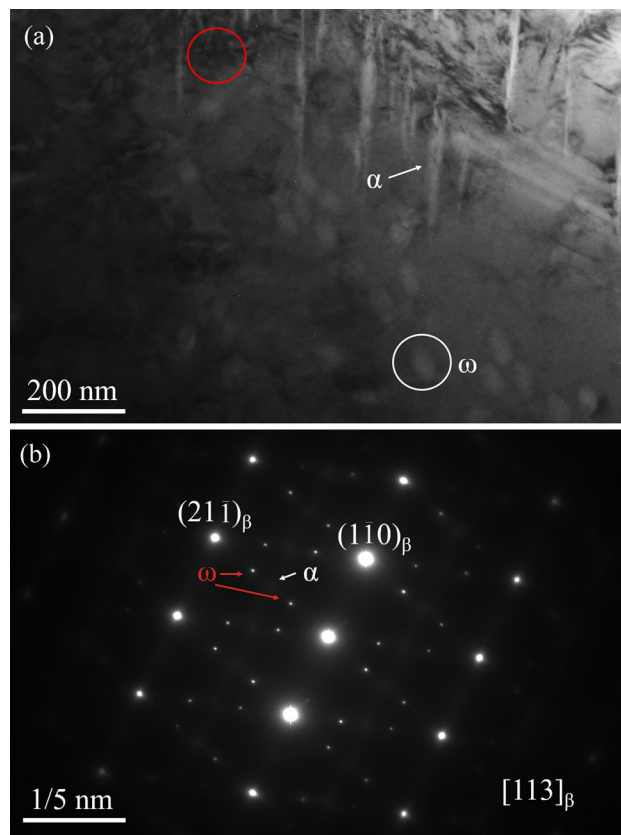


Fig. 7 (a) TEM imaging for cold-rolled TB8 alloy annealed at 450 °C and (b) the selected area electron diffraction pattern of $[113]_{\beta}$ zone

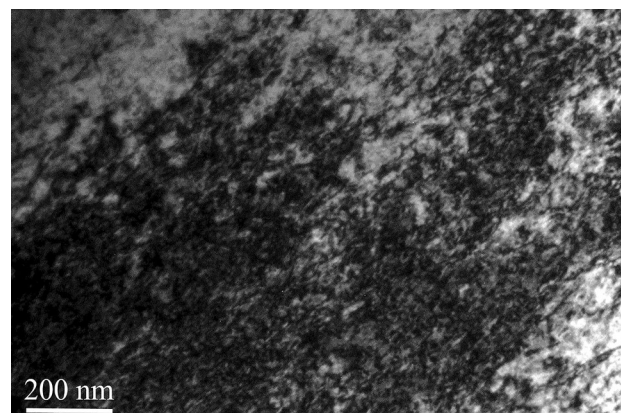


Fig. 8 TEM image of cold-rolled TB8 alloy plate

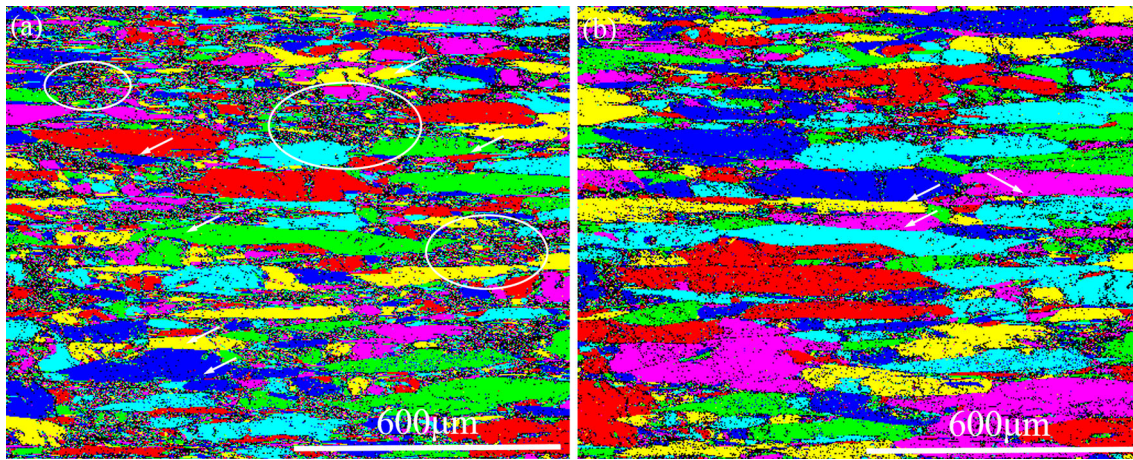


Fig. 9 EBSD grain micrographs of cold-rolled TB8 alloy annealed at 700 °C (a) misorientation angle more than 2° and (b) misorientation angle more than 15°

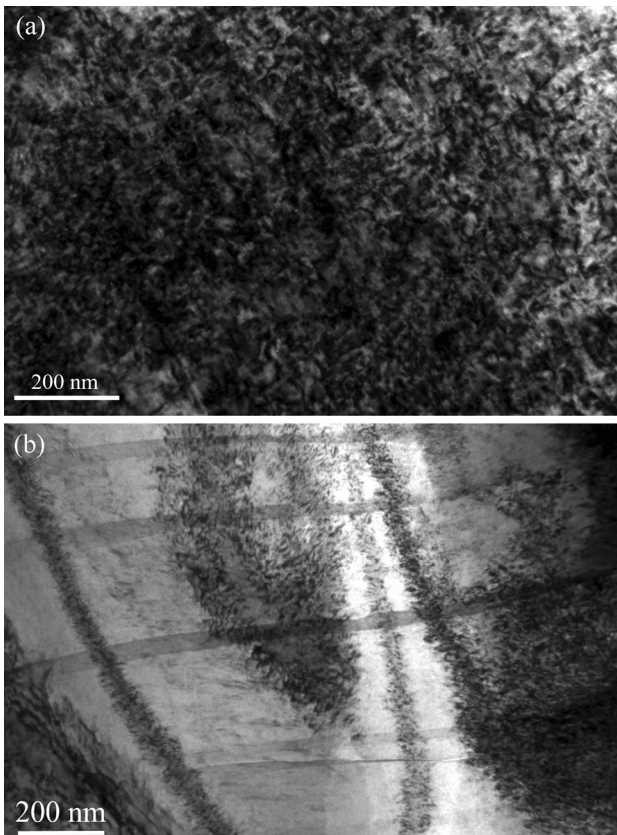


Fig. 10 TEM imaging for dislocations annealed at (a) 300 °C and (b) 750 °C

but decreases the elongation significantly. When the annealing temperature is 450 °C, α phase is formed (Fig. 7a), which further improves the strengthening of the alloy and forming larger ω phase, which makes the plasticity of the alloy still poor. When the annealing temperature is 500 and 550 °C, many fine α phases are formed, which shows a certain strengthening effect. At the same time, α phase and the matrix produce synergistic deformation, making the plasticity improved. Obvious softening process can be obtained when annealing temperature is above 600 °C. The enhancement effect was obviously

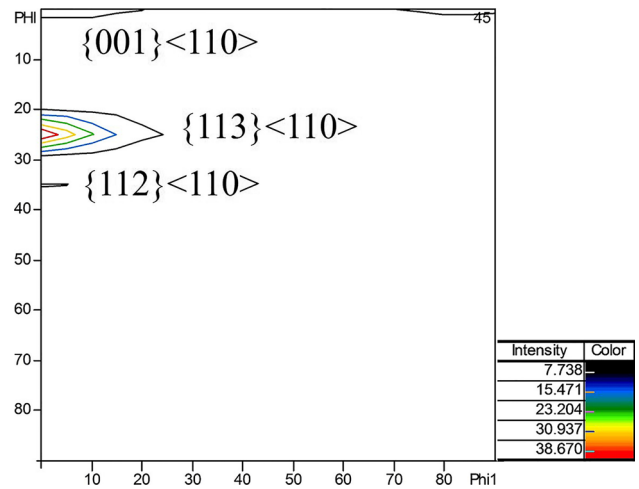


Fig. 11 Sections ($\phi_2 = 45^\circ$) of the orientation distribution functions (ODFs) of TB8 cold-rolled plate after annealed at 700 °C for 1 h

decreased as α phase grows up at 600 and 650 °C. When the annealing temperature is 700 °C or above, the amount of α phase is significantly less, which cannot play a significant role in strengthening. From the effect of microstructure transformation on mechanical properties, ω phase precipitation during annealing leads to the decrease of plasticity, and fine and uniform precipitation of α phase has obvious strengthening effect. When the α phase grows up, the strengthening effect decreases, and softening phenomenon appears after annealing above 550 °C due to the decrease in dislocation density.

3.4 Analysis of Tensile Fracture

Figure 12 manifests fracture morphologies of tensile samples annealing from 350 to 600 °C. There are amounts of rather deep ductile dimples, which results in its favorable plasticity when annealing at 350 °C, as seen in Fig. 12(a). When the annealing temperature is 400 °C (Fig. 12b), some elongated grains, as shown by the white arrow, exhibit quasi-cleavage fracture characteristics. The quasi-cleavage occurs in a local area, where dimples and tearing edges are connected to each

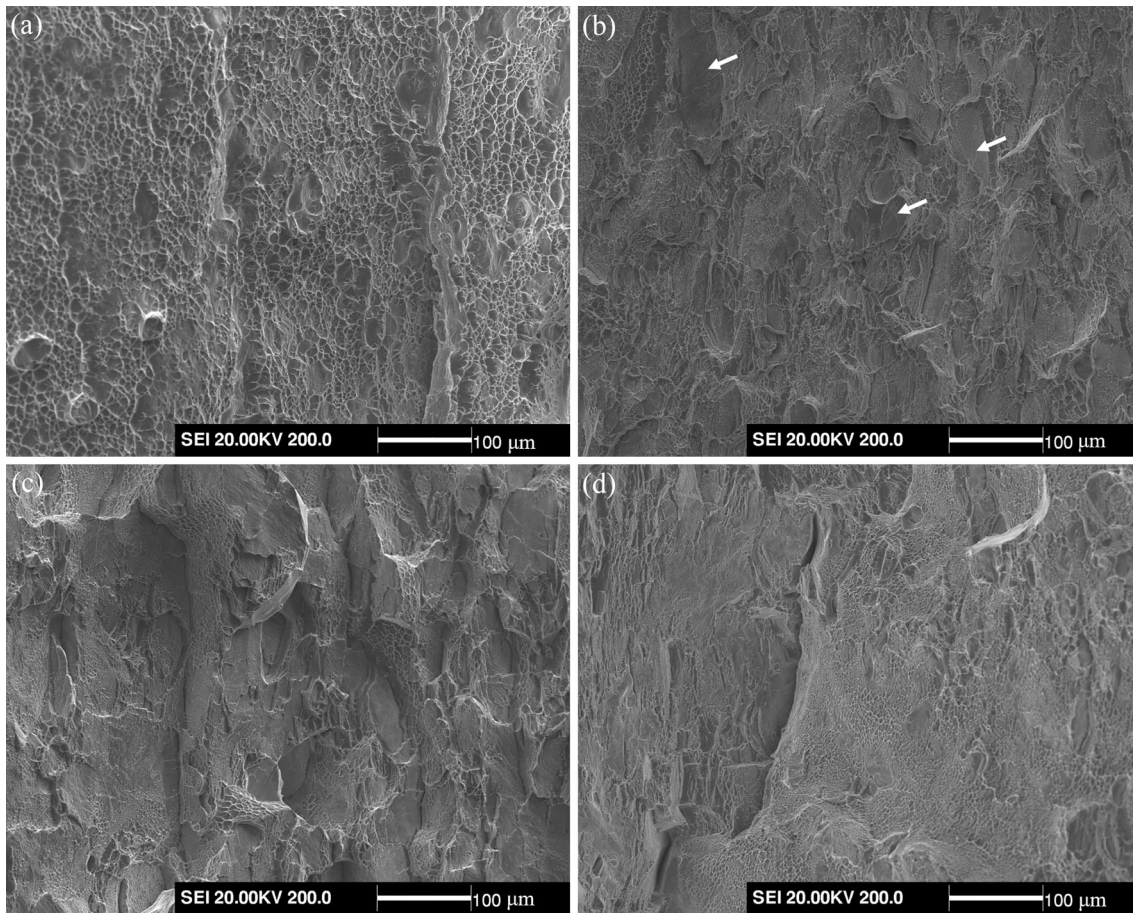


Fig. 12 Tensile fracture morphologies of TB8 cold-rolled plate annealed at (a) 350 °C (b) 400 °C (c) 550 °C and (d) 600 °C

other, showing a discernible brittleness. The appearance of this fracture feature is mainly attributed to the precipitation of ω phase. ω phase is a brittle phase, which promotes crack nucleation during tensile deformation. Small quasi-cleavage planes are formed during crack propagation. Because of the good plasticity of matrix, dimples connect the small cleavage planes. After annealing at 550 °C, the fracture represents mixed characteristics of transgranular fracture dimple and intergranular fracture with obvious tear characteristics, as shown in Fig. 12(c). When the annealing temperature is 550 °C, α phase is formed and interlaced, resulting in a large number of new α/β interfaces. Moreover, many dislocations are retained due to the low annealing temperature. In the tensile process, the phase interface hinders the dislocation movement, which makes the plasticity of materials low (Ref 34, 35). With the increase in annealing temperature, the dislocation density decreases and the plasticity of the material increases. Figure 12(d) illustrates the fracture morphology annealing at 600 °C. The fracture consists of transgranular dimple and tearing edge as well as the quasi-cleavage, and intergranular fracture disappear. Compared with the fracture annealed at 400 °C (Fig. 12b), the dimple size decreases, but plastic deformation increases obviously. Due to the presence of the growing α phase, there is a soft zone in the microstructure, which can be preferentially deformed in the tensile process, resulting in a relatively large plastic deformation in the relatively small region, providing a good plasticity (Ref 36, 37).

4. Conclusion

- (1) When the annealing temperature of cold-rolled TB8 plates with a thickness reduction of 50% is lower than 750 °C, recrystallization cannot occur, and the microstructure remains deformed characteristics, while considerable phase transition is found.
- (2) The ellipsoidal ω phase is formed when annealed at 400 °C, which result in a significant reduction in elongation. The orientation relationship between ω phase and β phase appears $\langle \bar{1}\bar{1}0 \rangle_{\beta} // \langle 11\bar{2} \rangle_{\omega}$ and $(1\bar{1}2)/(1\bar{1}00)$. When annealed from 450 to 750 °C, a large number of dislocations provide the nucleation sites of α phase. The size and volume fraction of α phase increases first and then declines in control of driving force of phase transformation and diffusion.
- (3) When the annealing temperature is below 750 °C, the main texture components are $\{001\} \langle 110 \rangle$, $\{113\} \langle 110 \rangle$, $\{112\} \langle 110 \rangle$, which remain almost the same as the cold-rolled state, indicating that the mechanical properties are largely determined by microstructure evolution and independent of texture.
- (4) The precipitation of ω and α phase occurs, and the large number of dislocations disappear, which provide a synergistic effect on the tensile strength and plasticity. The tensile strength of cold-rolled TB8 plates with a thickness reduction of 50% after annealing firstly decreases, then increases and finally decreases again with the in-

crease in annealing temperature, while the change in plasticity performs as increase–decline–increase.

Acknowledgment

This work was supported by Key Laboratory of Superlight Materials & Surface Technology (Harbin Engineering University), Ministry of Education; Application Technology Research and Development Program of Harbin under Grant (No.: 2017RAQXJ015).

References

1. J.F. Sun, Z.W. Zhang, M.L. Zhang, F.C. Jiang, and M.H. Ding, Microstructure Evolution and Their Effects on the Mechanical Properties of TB8 Titanium Alloy, *J. Alloys Compd.*, 2016, **663**, p 769-774
2. R.R. Boyer and R.D. Briggs, The Use of β Titanium Alloys in the Aerospace Industry, *J. Mater. Eng. Perform.*, 2015, **14**(6), p 681-685
3. J.C. Williams and E.A. Starke, Progress in Structural Materials for Aerospace Systems, *Acta Mater.*, 2003, **51**(19), p 5775-5799
4. S. Samuel, S. Nag, S. Nasrazadani, V. Ukirde, M.E. Bouanani, A. Mohandas, K. Nguyen, and R. Banerjee, Corrosion Resistance and In Vitro Response of Laser-Deposited Ti-Nb-Zr-Ta Alloys for Orthopedic Implant Applications, *J. Biomed. Mater. Res. Part A*, 2010, **94A**(4), p 1251-1256
5. R.S. Bedi, D.E. Beving, L.P. Zanella, and Y. Yan, Biocompatibility of Corrosion-Resistant Zeolite Coatings for Titanium Alloy Biomedical Implants, *Acta Biomater.*, 2009, **5**(8), p 3265-3271
6. K.X. Gu, B. Zhao, Z.J. Weng, K.K. Wang, H.K. Cai, and J.J. Wang, Microstructure Evolution in Metastable β Titanium Alloy Subjected to Deep Cryogenic Treatment, *Mater. Sci. Eng. A*, 2018, **723**, p 157-164
7. M.J. Lai, T. Li, and D. Raabe, ω Phase Acts as a Switch between Dislocation Channeling and Joint Twinning- and Transformation-Induced Plasticity in a Metastable β Titanium Alloy, *Acta Mater.*, 2018, **151**, p 67-77
8. T.W. Xu, J.S. Li, F.S. Zhang, F.Y. Wang, X.H. Liu, and Y. Feng, Microstructure Evolution during Cold-Deformation and Aging Response after Annealing of TB8 Titanium Alloy, *Rare Met. Mater. Eng.*, 2016, **45**(3), p 575-580
9. V. Hounkpati, S. Fréour, D. Gloaguen, V. Legrand, J. Kelleher, W. Kockelmann, and S. Kabra, In Situ Neutron Measurements and Modelling of the Intergranular Strains in the Near- β Titanium Alloy Ti- β 21S, *Acta Mater.*, 2016, **109**, p 341-352
10. B. Tang, B. Tang, F.B. Han, J.S. Li, and G.J. Yang, Hot Deformation Behavior of TB8 Alloy near the β -Transus, *Rare Met. Mater. Eng.*, 2013, **42**(9), p 1761-1766
11. T.W. Xu, J.S. Li, S.S. Zhang, F.S. Zhang, and X.H. Liu, Cold Deformation Behavior of the Ti-15Mo-3Al-2.7Nb-0.2Si Alloy and Its Effect on α Precipitation and Tensile Properties in Aging Treatment, *J. Alloys Compd.*, 2016, **682**, p 404-411
12. S.A. Mantri, D. Choudhuri, T. Alam, G.B. Viswanathan, J.M. Sosa, H.L. Fraser, and R. Banerjee, Tuning the Scale of α Precipitates in β -Titanium Alloys for Achieving High Strength, *Scr. Mater.*, 2018, **154**, p 139-144
13. S. Sadeghpour, S.M. Abbasi, M. Morakabati, L.P. Karjalainen, and D.A. Porter, Effect of Cold Rolling and Subsequent Annealing on Grain Refinement of a Beta Titanium Alloy Showing Stress-Induced Martensitic Transformation, *Mater. Sci. Eng. A*, 2018, **731**, p 465-478
14. M. Ahmed, D.G. Savvakis, O.M. Ivasishin, and E.V. Pereloma, The Effect of Thermo-Mechanical Processing and Ageing Time on Microstructure and Mechanical Properties of Powder Metallurgy near β Titanium Alloys, *J. Alloys Compd.*, 2017, **714**, p 610-618
15. Z.X. Du, S.L. Xiao, Y.P. Shen, J.S. Liu, J. Liu, L.J. Xu, F.T. Kong, and Y.Y. Chen, Effect of Hot Rolling and Heat Treatment on Microstructure and Tensile Properties of High Strength Beta Titanium Alloy Plates, *Mater. Sci. Eng. A*, 2015, **631**, p 67-74
16. B. Tang, H.C. Kou, X. Zhang, P.Y. Gao, and J.S. Li, Study on the Formation Mechanism of α Lamellae in a near β Titanium Alloy, *Prog. Nat. Sci. Mater. Int.*, 2016, **26**(4), p 385-390
17. A.R.V. Nunes, S. Borborema, L.S. Araújo, J. Dille, L. Malet, and L.H.D. Almeida, Production, Microstructure and Mechanical Properties of Cold-Rolled Ti-Nb-Mo-Zr Alloys for Orthopedic Applications, *J. Alloys Compd.*, 2018, **743**, p 141-145
18. S.J. Dai, Y. Wang, and F. Chen, Effects of Annealing on the Microstructures and Mechanical Properties of Biomedical Cold-Rolled Ti-Nb-Zr-Mo-Sn Alloy, *Mater. Charact.*, 2015, **104**, p 16-22
19. S. Dubinskiy, A. Korotitskiy, S. Prokoshkin, and V. Brailovski, In Situ X-ray Diffraction Study of a Thermal and Isothermal Omega-Phase Crystal Lattice in Ti-Nb-Based Shape Memory Alloys, *Mater. Lett.*, 2016, **168**, p 155-157
20. T. Li, D. Kent, G. Sha, L.T. Stephenson, A.V. Ceguerra, S.P. Ringer, M.S. Dargusch, and J.M. Cairney, New Insights into the Phase Transformations to Isothermal ω and ω -Assisted α in near β -Ti Alloys, *Acta Mater.*, 2016, **106**, p 353-366
21. R.F. Dong, J.S. Li, J.K. Fan, H.C. Kou, and B. Tang, Precipitation of α Phase and Its Morphological Evolution during Continuous Heating In A Near β Titanium Alloy Ti-7333, *Mater. Charact.*, 2017, **132**, p 199-204
22. X. Zhang, H.C. Kou, J.S. Li, F.S. Zhang, and L. Zhou, Evolution of the Secondary α Phase Morphologies during Isothermal Heat Treatment in Ti-7333 Alloy, *J. Alloys Compd.*, 2013, **577**, p 516-522
23. L. Mora, C. Quesne, and R. Penelle, Relationships among Thermo-mechanical Treatments, Microstructure, and Tensile Properties Of A Near Beta-Titanium Alloy: β -CEZ: Part II. Relationships between Thermo-mechanical Treatments and Tensile Properties, *J. Mater. Res.*, 1996, **11**, p 89-99
24. Z.X. Du, S.L. Xiao, L.J. Xu, J. Tian, F.T. Kong, and Y.Y. Chen, Effect of Heat Treatment on Microstructure and Mechanical Properties of a New β High Strength Titanium Alloy, *Mater. Des.*, 2014, **55**, p 183-190
25. F. Langmayr, P. Fratzl, G. Vogl, and W. Miekeley, Crossover from Omega-Phase to Alpha-Phase Precipitation in BCC Ti-Mo, *Phys. Rev. B Condens. Mater. Phys.*, 1994, **49**(17), p 11759-11766
26. D.L. Moffat and D.C. Larbalestier, The Competition between the α and Omega Phases in Aged Ti-Nb Alloys, *Metall. Trans. A*, 1988, **19**(7), p 1687-1694
27. D.H. Ping, Review on ω Phase in Body-Centered Cubic Metals and Alloys, *Acta Metall. Sin. (Engl. Lett.)*, 2014, **27**(1), p 1-11
28. A. Lasalmonie and C. Chaix, Heterogeneous Precipitation of the ω Phase in a β Titanium Alloy, *Philos. Mag. A*, 1981, **44**(4), p 973-981
29. X.D. Zhang, J.M.K. Wiezorek, W.A. Baeslack, III, D.J. Evans, and H.L. Fraser, On the Stability of ω Phase in Ti-6-22-22S and Ti-6-4 Alloys, *Scr. Mater.*, 1999, **41**(6), p 659-665
30. T. Yamane and J. Ueda, Tempering Behavior of a Ti-Cr Alloy Quenched from β Region, *Trans. Jpn. Inst. Met.*, 1965, **6**(3), p 151-153
31. Y. Ohmori, T. Ogo, K. Nakai, and S. Kobayashi, Effects of ω -Phase Precipitation on $\beta \rightarrow \alpha$, α'' Transformations in a Metastable β Titanium Alloy, *Mater. Sci. Eng. A*, 2001, **312**(1), p 182-188
32. S. Nag, R. Banerjee, R. Srinivasan, J.Y. Hwang, M. Harper, and H.L. Fraser, ω -Assisted Nucleation and Growth of α Precipitates in the Ti-5Al-5Mo-5V-3Cr-0.5Fe β Titanium Alloy, *Acta Mater.*, 2009, **57**(7), p 2136-2147
33. R.F. Dong, J.S. Li, H.C. Kou, J.K. Fan, and B. Tang, Dependence of Mechanical Properties on the Microstructure Characteristics of a near β Titanium Alloy Ti-7333, *J. Mater. Sci. Technol.*, 2019, **34**(1), p 48-54
34. G. Lütjering, J. Albrecht, C. Sauer, and T. Krull, The Influence of Soft, Precipitate-Free Zones at Grain Boundaries in Ti and Al Alloys on Their Fatigue and Fracture Behavior, *Mater. Sci. Eng. A*, 2007, **468**(1), p 201-209
35. L. Lilensten, Y. Danard, C. Brozek, S. Mantri, P. Castany, T. Gloriant, P. Vermaut, F. Sun, R. Banerjee, and F. Prima, On the Heterogeneous Nature of Deformation in a Strain-Transformable Beta Metastable Ti-V-Cr-Al Alloy, *Acta Mater.*, 2019, **162**, p 268-276
36. C. Sauer and G. Lütjering, Influence of α Layers at β Grain Boundaries on Mechanical Properties of Ti-Alloys, *Mater. Sci. Eng. A*, 2001, **319**(01), p 393-397
37. B. Song, W.L. Xiao, C.L. Ma, and L. Zhou, Influence of Phase Transformation Kinetics on the Microstructure and Mechanical Properties of near β Titanium Alloy, *Mater. Charact.*, 2019, **148**, p 224-232

Publisher's Note Springer Nature remains neutral with regard to jurisdictional claims in published maps and institutional affiliations.